Heliyon 10 (2024) e38533

Contents lists available at ScienceDirect

Heliyon

journal homepage: www.cell.com/heliyon

Research article

How to improve drought resilience to guarantee regional sustainable development

Huihui Wang [a,b,c,*], Xiaoyong Gao [a,d,e,**], Yunsong Yang [a,b], Zhengzao Wang [f], Shuhong You [a,g], Hanyu Xue [a,g,h], Wanlin He [a,g]

[a] Advanced Institute of Natural Sciences, Beijing Normal University, Zhuhai, 519087, China
[b] School of Environment, Beijing Normal University, Beijing, 100875, China
[c] Key Laboratory of Coastal Water Environmental Management and Water Ecological Restoration of Guangdong Higher Education Institutes, Beijing Normal University, Zhuhai, 519087, China
[d] Department of Geography, National University of Singapore, Singapore, 117570, Singapore
[e] Huitong College, Beijing Normal University, Zhuhai, 519087, China
[f] School of Economics and Management, Beijing University of Technology, Beijing, 100124, China
[g] Zhixing College, Beijing Normal University, Zhuhai, 519087, China
[h] Research Institute of Urban Renewal, Zhuhai Institute of Urban Planning and Design, Zhuhai, 519100, China

A R T I C L E I N F O

Keywords:
Drought resilience
Sustainable development
Spatial-temporal evolution
Influencing factors
BP neural network

A B S T R A C T

Drought is a pressing environmental issue with profound socio-economic impacts. Frequent drought disasters around the world have brought huge impacts and challenges, severely constraining the sustainable development of cities. How to improve drought resilience to guarantee regional sustainable development has become a hot research topic. In this study, we developed a comprehensive framework to assess drought resilience in China, analyzing its spatiotemporal evolution characteristics, uncovering the underlying impact mechanisms, and projecting future resilience trends across different regions of the country. Over the past 12 years, the average drought resilience level in China has risen by 14.4 %. Central and eastern coastal provinces demonstrated higher resilience levels, contrasting with the western inland regions' lower resilience. A significant positive spatial correlation was observed in China's drought resilience, with high-value clusters emerging in the southeastern and northeastern regions. Among the sub-resilience dimensions, social resilience had the most substantial impact. The prediction model suggests that the drought resilience level will increase modestly by 6.2 % across provinces, maintaining the spatial pattern of higher resilience in the eastern coastal areas and the southern and northern extremities, with lower resilience in the central region. Our findings underscore the significance of understanding regional variations in drought resilience to inform targeted and efficient policy interventions.

Notes

The authors declare no competing financial interest.

* Corresponding author.
** Corresponding author.
E-mail addresses: wanghui@bnu.edu.cn (H. Wang), 201911039071@mail.bnu.edu.cn (X. Gao).

https://doi.org/10.1016/j.heliyon.2024.e38533
Received 3 October 2023; Received in revised form 24 August 2024; Accepted 25 September 2024
Available online 26 September 2024

1. Introduction

Drought is an intricate natural disaster that has profound impacts on agriculture [1], ecology [2], and the economy [3], among other sectors. According to the Sixth Assessment Report (AR6) of the Intergovernmental Panel on Climate Change (IPCC), drought has negatively impacted food systems, agriculture, forestry, fisheries, and the production capacity of agricultural products, exacerbating global food security and nutrition challenges while also having severe effects on ecosystems and human health [4,5]. From an international perspective, the economic losses caused by droughts are colossal, surpassing tens of billions of dollars annually, more than other climate-related disasters [6]. With the progression of climate change, both the frequency and intensity of droughts are expected to escalate. Positioned between the Eurasian continent and the Pacific Ocean, China is influenced by the East Asian monsoon climate. This results in abundant rainfall during the summer and cold, dry conditions in the winter. The instability of the monsoon exacerbates these conditions. Historically, from 206 BCE to 1949, China experienced 1056 drought events [7]. Furthermore, about 6.9229 million people and 3.681 million heads of large livestock confronted water access difficulties due to droughts [8]. Being the world's largest developing country, China's burgeoning population and rapid urbanization have heightened water demand, amplifying the potential adverse impacts of droughts [9].

Owing to the intricacy and multifaceted nature of drought risk, it cannot be characterized solely by singular indicators like insufficient rainfall [10]. Such risk is typically driven by a myriad of underlying and specific determinants, encompassing environmental, social, economic, cultural, and governance dimensions [11]. Presently, research on drought disasters predominantly centers on vulnerability. Vulnerability delineates the susceptibility or predisposition of systems and their constituents to harm, coupled with a deficiency in short-term coping capacities and long-term adaptive mechanisms, resulting in adverse implications [10]. Vulnerability and resilience are two interconnected yet distinct notions; vulnerability often serves as an instrument for risk appraisal, while resilience encapsulates overarching objectives and inherent attributes. Vulnerability underscores the pre-disaster state of a system, namely its latent propensity for harm [12], whereas resilience is a dynamic process focusing on both during and post-disaster phases, bolstering the system's disaster resistance capabilities [13]. Current drought investigations primarily concentrate on exposure and sensitivity, with scant emphasis on the recuperative aspects of urban systems post-disaster or a systemic incorporation thereof [14]. Confronted with analogous drought challenges, diverse research orientations yield varying outcomes, indicating that a universal vulnerability assessment system for urban droughts is elusive. Given the circumscribed reference value vulnerability offers for urban planning, specialized studies on urban drought resilience can furnish policymakers with robust theoretical underpinnings, aiding them in effectively tackling urban drought challenges.

Research into urban resilience is instrumental in addressing drought challenges. Urban resilience is defined as the capacity of a city to resist and/or adapt to specific disturbances, reinstating its typical functions or equilibrium state [15]. This concept was initially introduced by the International Council for Local Environmental Initiatives (ICLEI) in 2002, advocating for enhanced research into urban disaster resilience. The Fifth Plenary Session of the 19th Central Committee of the Communist Party of China in 2020 also championed the construction of resilient cities, reflecting contemporary paradigms and trajectories in urban development. In light of potential drought risks, augmenting the defensive capabilities of urban systems has become paramount. Given the intricate interplay between social and natural systems, resource and environmental challenges are frequently perceived as complex systemic issues [16]. Against this backdrop, synthesizing interactions among economic, social, institutional, and natural systems to evaluate and bolster urban resilience not only equips us to adeptly confront shifts and shocks but also emerges as pivotal for sustainable development. Current research on drought resilience is chiefly qualitative, predominantly involving interviews and policy discourse [17–21]. Vinh et al. employed remote sensing (RS) and Geographic Information Systems (GIS) to investigate how land use and cover changes drive urban drought resilience in Ninh Thuan, Vietnam [22]. Cai et al. quantified flood occurrences, drought severity, and associated disaster resilience across 81 cities in mainland China by formulating a resilience index [23]. Nonetheless, the data and methodologies employed in this study are somewhat rudimentary and fall short of providing an efficacious assessment of drought resilience. Existing drought resilience research has gaps at the provincial scale. For China, a country with vast geographical variations and a plethora of climatic types, a systematic assessment of provincial drought resilience is of paramount significance. This facilitates a more nuanced comprehension of the coping capacities and latent risks of different provinces under drought conditions. Specific to each province, policymakers, decision-makers, and local communities can devise tailored, targeted strategies and interventions based on these research findings, with the aim of bolstering their drought resilience and mitigating the adverse impacts of drought.

In this study, we established a drought resilience assessment framework based on "Social-Economic-Environmental-Institutional" dimensions. Grounded in this framework, the entropy-weighted TOPSIS method was employed to measure China's drought resilience, with the Theil index being used to analyze its spatial-temporal heterogeneity. Subsequently, the Global Moran's index and Getis-Ord Gi* Index were employed to elucidate the dependency and hotspot regions of China's drought resilience. Further, the influence of sub-resilience on drought resilience was explored utilizing a structural equation model. For the upcoming 14 years, the BP neural network was meticulously employed to project the intricate trends and potential shifts in drought resilience. Through this research, we addressed the following questions: (1) What is the degree of drought resilience in China? (2) What is the nature of the spatial-temporal heterogeneity and dependency of drought resilience? (3) How does sub-resilience influence China's drought resilience? (4) What are the potential alterations in China's drought resilience over the next 14 years? We aspire that these profound studies and discoveries will foster the refinement and updating of strategies, concentrating on holistically enhancing drought resilience and diminishing provincial disparities, thereby offering a replicable blueprint for the global arena.

2. Materials and methods

2.1. Study area

China, situated in East Asia and spanning approximately 9.6 million square kilometers, is a nation characterized by its intricate and diverse geographical landscapes. Notably, regions in the northwest, such as Xinjiang and Qinghai, despite their vast expanses, have a relatively sparse population due to their arid climatic conditions. In contrast, the eastern coastal regions, blessed with a humid climate, are not only densely populated but also economically prosperous (Fig. 1). In response to the detrimental effects of aridity on agriculture, the Chinese government has instituted a myriad of strategies, encompassing water conservation initiatives and the promotion of renewable energy technologies. These strategies are designed to ensure sustainable economic and societal advancement across the nation's territories.

2.2. Methodology

2.2.1. Methodological framework

Drought disasters have imparted significant adverse impacts on societies, severely impeding urban sustainable development. Enhancing urban resilience against drought to foster sustainable growth has emerged as a focal point of research. China frequently grapples with severe droughts, leading to substantial economic losses. Evaluating the drought resistance capabilities of various Chinese provinces and discerning the influencing factors aids the government in the judicious allocation of disaster relief funds, bolstering regional disaster resilience to promote regional sustainable development. To investigate how to improve drought resilience to guarantee regional sustainable development, this study introduces an assessment framework for drought resistance capabilities based on "Social-Economic-Environmental-Institutional" (Fig. 2). Grounded in this framework, we established an evaluation structure for drought resistance capabilities encompassing the "Social-Economic-Environmental-Institutional" dimensions. Within this structure, the entropy-weighted TOPSIS method was employed to calculate China's drought resistance capabilities, followed by the application of the Theil index to analyze its spatiotemporal heterogeneity. Subsequently, the Global Moran's index and Getis-Ord Gi* index were utilized to elucidate the dependencies and hotspot regions of China's drought resistance capabilities. Moreover, the structural equation model was employed to explore the influence of sub-resilience on drought recovery capabilities. Over the subsequent 14 years, the BP neural network was meticulously applied to forecast the intricate trends and potential shifts in drought resistance capabilities, culminating in the proposition of pertinent policy recommendations.

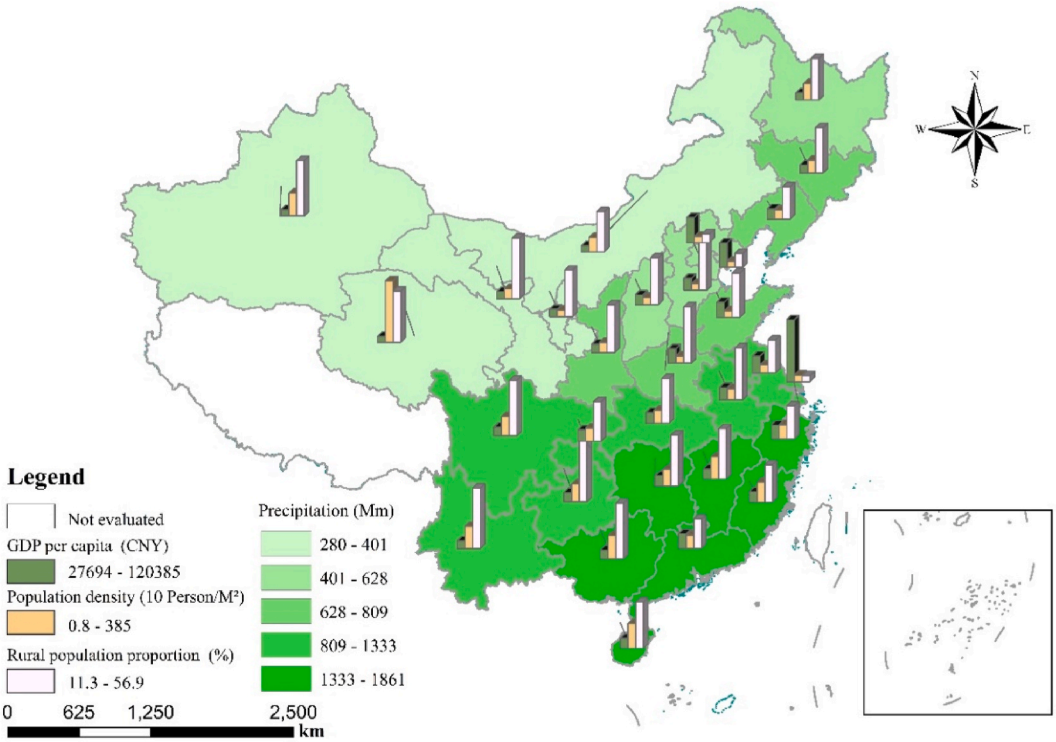

Fig. 1. The study area of China.

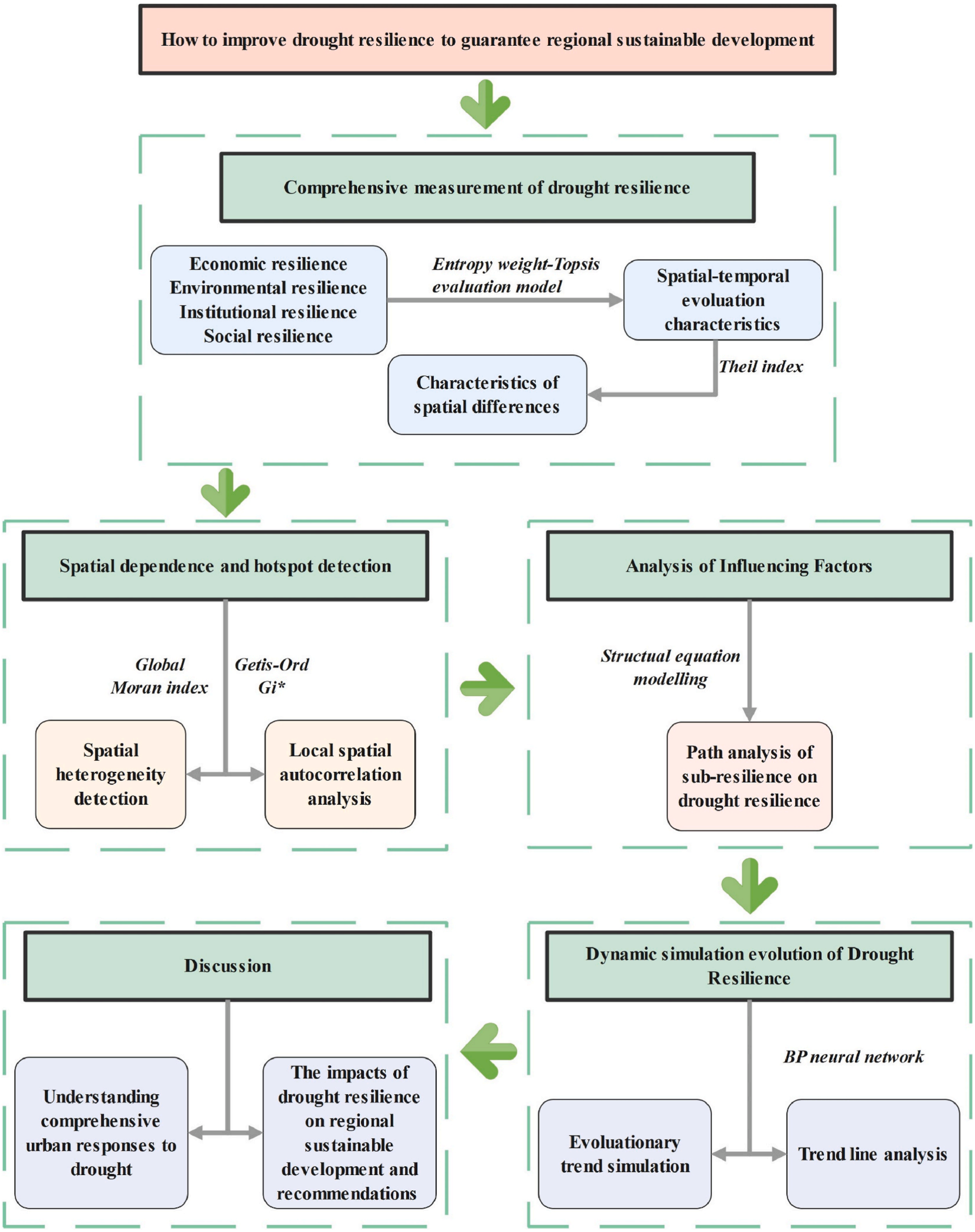

Fig. 2. The method framework for this study.

2.2.2. *Indicator system construction*

In this study, indicators were preliminarily selected from various aspects, including economic level, environment, institution, and social factors. During the initial development of the comprehensive evaluation index system for drought resilience, a large number of indicators were pre-selected, and basic data spanning 12 years were collected. Correlation analysis was then conducted on these pre-selected indicators. Relevant tests were performed using SPSS 20.0 software to examine the constructed assessment index system, aiming to eliminate redundant evaluation indicators that reflect similar information. Consequently, under the premise of aligning with urban resilience and disaster resilience theories, the most feasible indicators were screened to establish a drought resilience system evaluation framework. A total of 23 evaluation indicators were selected for the drought resilience assessment system (Table 1).

Table 1
Evaluation index system of drought resilience.

Criterion layer	Indicator layer	Indicator units and properties	Evaluation content
Economic resilience (EcoR)	X_1: The proportion of agriculture in GDP (−)	%	Economic diversification
	X_2: GDP per capita (+)	CNY	Economic development
	X_3: Per capita net income of rural residents (+)	CNY	Rural income level
	X_4: Per Capita Grain Production (+)	ton/person	Agricultural productivity
	X_5: GDP per unit of water (−)	CNY/Ton	Water use efficiency
Environmental resilience (EnvR)	X_6: Forest Coverage (+)	%	Environmental sustainability
	X_7: Average annual temperature (−)	celsius	Temperature variability
	X_8: Average annual precipitation (+)	mm	Water availability
	X_9: Average annual sunshine (−)	h	Sunshine time
Institutional resilience (IR)	X_{10}: Small reservoir capacity (+)	cubic meters/square kilometer	Water storage capacity
	X_{11}: Fertilizer application per unit area (+)	ton/mu	Agricultural productivity
	X_{12}: Number of beds in medical institutions per thousand: people (+)	Number of beds/ 1000people	Healthcare infrastructure
	X_{13}: Effective irrigation rate (+)	%	Irrigation efficiency
	X_{14}: Coverage of green areas in the jurisdiction (+)	%	Green area coverage.
	X_{15}: sewage treatment rate (+)	%	Sewage treatment efficiency.
Social resilience (SR)	X_{16}: Proportion of urban residents enrolled in social insurance at the end of the year (+)	%	Social insurance enrollment rate.
	X_{17}: Proportion of rural population to total population (−)	%	Urbanization level
	X_{18}: Population density (−)	10,000 people/square kilometer	Population distribution
	X_{19}: Registered urban unemployment rate at the end of the year (−)	%	Labor market conditions
	X_{20}: Per capita daily domestic water consumption (−)	liters/person	Water conservation awareness
	X_{21}: Proportion of illiterate and semi-literate individuals aged 15 and above (−)	%	Literacy rate.
	X_{22}: Proportion of staff in higher education institutions. (+)	%	Higher education institution staff ratio
	X_{23}: Proportion of population aged below 15 and above 65(−)	%	Age dependency ratio

2.2.3. Entropy weight-TOPSIS evaluation model

This section employs the entropy weighted-TOPSIS approach for a comprehensive evaluation of drought resilience and sub-resilience in China. Developed by Hwang and Masud [24] in 1981, TOPSIS stands as a widely adopted method for integrated assessments. The entropy-TOPSIS method is a multi-criteria decision-making approach that integrates the entropy-weighting technique with the TOPSIS model. This approach is an enhanced evaluation method that builds on the TOPSIS model by incorporating entropy weighting [25–28]. The core principle involves assessing the distance between the evaluated object and the best or worst possible values, then calculating the closeness of the object to the ideal value to rank its strengths and weaknesses. The entropy-weighted TOPSIS model is favored for its simplicity, objectivity, low sample size requirements, and ability to generate reasonable and reliable results. This method effectively leverages the information in the original data to compute the utility values of each indicator and objectively determine the weights. Using these weights derived from the entropy weighting method, the TOPSIS model is then constructed by calculating the weighted Euclidean distances between the positively normalized original values and both the ideal and anti-ideal values, ultimately determining the drought resilience level of each region. The main steps of the entropy weight-TOPSIS method are as follows:

Establish the matrix X, which is an n*m matrix representing n provinces and m indicators.

$$X = [X_{ij}]_{n\times m}, i = 1, 2, 3, \cdots, n, j = 1, 2, 3, \cdots, m \tag{1}$$

To eliminate the influence of different variable magnitudes and units, all indicator variables were subjected to a process of standardization. Due to the varying impacts of different indicators on the outcome, two different methods of standardization were employed.

$$\begin{cases} x'_{ij} = \dfrac{x_{ij} - \min\{x_{1j}, \cdots, x_{mj}\}}{\max\{x_{1j}, \cdots, x_{mj}\} - \min\{x_{1j}, \cdots, x_{mj}\}}, i \in [1, m], j \in J_1 \\ x'_{ij} = \dfrac{\max\{x_{1j}, \cdots, x_{mj}\} - x_{ij}}{\max\{x_{1j}, \cdots, x_{mj}\} - \min\{x_{1j}, \cdots, x_{mj}\}}, i \in [1, m], j \in J_2 \end{cases} \tag{2}$$

where J_1 represents positive indicators, indicating that these variables have a positive impact on drought resilience. Conversely, J_2 represents negative indicators, signifying that these variables have a negative impact on resilience. x'_{ij} denotes the standardized evaluation value.

Transform matrix X into a trend-consistent matrix X' by applying the same trend method. Normalize (**Eq. (3)**) the indicators to obtain matrix A.

$$A = [a_{ij}]_{n\times m},\ a_{ij} = X'_{ij} \Bigg/ \sqrt{\sum_{i=1}^{n} \left(X'_{ij}\right)^2} \tag{3}$$

Use the entropy weight method to determine the weights w of each indicator in the drought resilience system (Table S1).

$$w_j = \frac{1 - e_j}{m - \sum_{j=1}^{m} e_j} \tag{4}$$

In this method, $e_j = -\frac{1}{\ln n}\sum_{i=1}^{n} f_{ij} \ln f_{ij}$ represents the information entropy, while f_{ij} represents the weight of each indicator value.

Determine the positive and negative ideal solutions based on the matrix.

$$A^{\pm} = \left(a_{i1}^{\pm}, a_{i2}^{\pm}, a_{i3}^{\pm}, \dots, a_{im}^{\pm}\right) \tag{5}$$

Calculate the Euclidean distance between each indicator value and the ideal solution.

$$D_i^{+} = \sqrt{\sum_{j=1}^{m} w_j \left(a_{ij}^{+} - a_{ij}\right)^2}$$
$$D_i^{-} = \sqrt{\sum_{j=1}^{m} w_j \left(a_{ij}^{-} - a_{ij}\right)^2} \tag{6}$$

Calculate the closeness degree between each evaluation object and the ideal solution.

$$C_i = \frac{D^-}{D^+ + D^-} \tag{7}$$

2.2.4. Global Moran's index

We examine the spatial autocorrelation of drought resilience in China using the global Moran index. Spatial autocorrelation is an essential method for studying spatial distribution. Spatial autocorrelation statistics reflect the potential level of dependence among elements with different geographical locations [29]. Currently, the Moran's Index is the primary indicator used to measure spatial autocorrelation. Its values range from −1 to 1, with values > 0 indicating positive spatial correlation, and values < 0 indicating negative spatial correlation [30]. In this study, we utilized the spatial autocorrelation analysis tool in GeoDa 1.16 software to analyze the spatial correlation of drought resilience [31]. Considering the geographic characteristics of the research units, this study selects the Rook adjacency spatial weight matrix to measure the values of Moran's Index. This means that if there is an adjacent boundary between any two provinces, they are considered neighbors. As Hainan Province is geographically independent from the Chinese mainland, this study designates Guangdong Province, which is closest to Hainan Province, as its adjacent province.

The formula for calculating Moran's I is as follows:

$$Moran's\ I = \frac{n\sum_{i}\sum_{j} W_{ij}(x_i - \bar{x})(x_j - \bar{x})}{S_0\sum_{i}(x_i - \bar{x})^2}, i, j = 1, 2, \cdots, n \tag{8}$$

where $S_0 = \sum_i\sum_j W_{ij}$, where W_{ij} represents an element in the spatial adjacency matrix W, x_i and x_j represent the values of drought resilience in provinces i and j respectively. $\bar{x}$ represents the mean value of drought resilience, n represents the total number of provinces.

When the absolute value of the *Moran's I* test statistic $Z(I)$ is greater than 1.96, $P < 0.05$, it indicates statistical significance and the null hypothesis is rejected, implying that the spatial distribution of the attributes is in a clustered state. If the absolute value of the *Moran's I* test statistic $Z(I)$ is less than 1.96, then $P > 0.05$, indicating no statistical significance and accepting the null hypothesis, indicating that the spatial distribution of attributes tends to be random.

2.2.5. Getis-Ord Gi* index

The Getis-Ord Gi* index is called "hot and cold analysis" and used to identify high- and low-value clusters of spatial unit elements [32–35]. This study analyzes the significance of Z(Gi*) and typically classifies it into hotspots, cold spots, and non-significant regions to identify the spatial distribution of different drought resilience levels in Chinese provinces.

The formula for calculation is as follows:

$$G_i^* = \sum_{j=1}^{n} W_{ij}X_j \Bigg/ \sum_{j=1}^{n} X_j \tag{9}$$

$$Z(G_i^*) = \frac{G_i^* - E(G_i^*)}{\sqrt{Var(G_i^*)}} \tag{10}$$

where Z(Gi*) is the standardized statistical measure used to test its significance. n represents the number of provinces, X_j represents the drought resilience value of spatial units j, and W_{ij} represents the spatial weight matrix. $Z(G_i^*)$ represents the Z test value, where $E(G_i^*)$ denotes the mean and $Var(G_i^*)$ represents the variance.

If the G_i^* value is positive and significant, it indicates a clustering of high values in the vicinity of the spatial unit. Conversely, if the G_i^* value is negative and significant, it suggests a clustering of low values in the vicinity of the spatial unit. Therefore, this method can detect whether there is a clustering of high or low values [36].

2.2.6. Theil index

Theil index is initially proposed based on information theory and generated from generalized entropy measure [37,38]. In this study, the Theil index method is employed to analyze the disparities in drought resilience among provinces in China, including the national level and the eastern, central, western, and northeastern regions. (Following the traditional division of China's four major economic regions, the eastern region includes Beijing, Tianjin, Hebei, Shanghai, Jiangsu, Zhejiang, Fujian, Shandong, Guangdong, and Hainan; the central region includes Shanxi, Anhui, Jiangxi, Henan, Hubei, and Hunan; the western region includes Guangxi, Chongqing, Sichuan, Guizhou, Yunnan, Shaanxi, Gansu, Qinghai, Ningxia, Xinjiang, and Inner Mongolia; the northeastern region includes Liaoning, Jilin, and Heilongjiang). The Theil index representing drought resilience in China is presented in this study as follows:

$$\begin{aligned} T_t &= \frac{1}{n}\sum_{i=1}^{n}\frac{R_i}{\overline{R}}\ln\left(\frac{R_i}{R}\right) \\ T_t &= T_{wt} + T_{bt} \\ T_w &= \sum_{p=1}^{m}\left(\frac{n_p}{n}\frac{\overline{e}_p}{\overline{e}}\right)T_p \\ T_b &= \sum_{p=1}^{m}\left(\frac{n_p}{n}\frac{e_p}{\overline{e}}\right)\ln\left(\frac{e_p}{\overline{e}}\right) \end{aligned} \tag{11}$$

where i represents provinces, and t represents years. R_i represents the drought resilience of province i, and $\overline{R}_t$ represents the average drought resilience of all provinces in year t; T_t、 T_{wt} and T_{bt} represent the Theil index for the entire region in year t, the Theil index within regions in year t and the Theil index between regions in year t; n_p is the number of provinces in group p, $\overline{e}_p$ is the average index value of group p, and $\overline{e}$ is the average index value of all provinces. T_p represents the Theil index of group p.

2.2.7. Structural equation model

In this study, an exploratory structural equation model (ESEM) was employed to analyze the interaction between drought resilience in China and subdomain resilience. It is also known as Covariance Structure Modeling. Structural equation model (SEM) can examine the relationships between latent variables and observed variables, as well as the causal relationships within latent variable paths, measuring the degree of influence between variables or the effects of variables [39,40]. To investigate the interaction between drought resilience and its sub-domain resilience, an exploratory SEM analysis is conducted to examine the influencing factors of drought resilience in China. Generally, it is recommended to have a sample size of at least 100 to 150 for estimating structural models using the maximum likelihood (ML) method [41]. In this study, the drought resilience data of 30 provinces (municipalities, autonomous regions) in China from 2010 to 2021 are selected as the research sample, resulting in a total of 360 observations. Therefore, the sample size meets the minimum requirements and is suitable for structural equation modeling.

The AMOS 24 software is utilized in this study to construct the model and conduct measurement analysis [42–45]. The most effective indicator to assess the fit between the research model and the statistical data is the goodness of fit. As shown in Table S2, the model fit indices fall within the recommended range, indicating that the model is appropriate.

2.2.8. BP neural network

The backpropagation neural network is the most successful and extensively used artificial neural network [46–48]. It is a type of multi-layer feedforward neural network commonly employed for classification and regression tasks. This neural network consists of an input layer, an output layer, and one hidden layer.

We take a three-layer (including one hidden layer) backpropagation (BP) network as an example to introduce (Fig. S1). The input data is denoted as X, the parameters from the input layer to the hidden layer are represented by w and b1. Similarly, the parameters from the hidden layer to the output layer are represented by v and b2. The activation functions used are g1 for the hidden layer and g2 for the output layer. Therefore, the model can be defined as follows:

Input layer to hidden layer:

$$\mathrm{net}_1 = w^T x + b_1, h = g_1(\mathrm{net}_1) \tag{12}$$

Hidden layer to output layer:

$$\mathrm{net}_2 = v^T h + b_2, \hat{y} = g_2(\mathrm{net}_2) \tag{13}$$

model:

$$\hat{y} = g_2(\ \mathrm{net}_2) = g_2\left(v^T g_1(\mathrm{net}_1) + b_2\right) = g_2\left(v^T g_1\left(w^T x + b_1\right) + b_2\right) \tag{14}$$

In this study, we used a Backpropagation (BP) neural network to simulate drought resilience levels in Chinese provinces from 2022 to 2035. We used Python 3.9 and the machine learning library torch.nn's Module class to construct the feedforward neural network [49,50]. The training samples consisted of indicator data collected from 2010 to 2021. The data was split into a training set (2010–2015) and a test set (2016–2021). To eliminate the differences in the data, we normalized all training data. Specifically, during training, we used historical data for each indicator from the past 5 years as input to predict the value of that indicator for the next year. Therefore, the input layer node size $n = 5$, the time window size is 1, and the output layer node size $m = 1$; The number of hidden layer nodes $n_1 = \sqrt{n+m} + C$, C ranging from 1 to 10, corresponding to a range of 4–13. Based on the MSE (mean squared error) values from the tuning process, we determined that the optimal hidden layer size is 1 with 3 neurons. The initial learning rate $\eta(0) = 0.05$, the error precision $\varepsilon = 0.001\%$, and the number of iterations $M_0 = 100$. The *Sigmoid* function is chosen as the activation function, while the remaining parameters are set to their default values. Finally, using historical data from 2010 to 2021, we trained the model to predict the values of indicators for the years 2022–2035.

However, given the limited sample size in predicting drought resilience levels, the resulting predictions may not be highly convincing. To improve the reliability of these predictions, it's crucial to assess the model's performance. Cross-validation is particularly useful in such cases, especially when the dataset is small. The 5-fold Cross-Validation method is commonly used in machine learning and data mining to evaluate model accuracy [51], and is well-established as a robust statistical tool for model evaluation [52]. In this study, we further used 5-fold Cross-Validation with the scikit-learn library in Python to confirm the reliability of our predictions [53,54].

2.3. Data sources

The specified geographical scope for data collection in this study is the 30 provincial-level administrative regions of China, excluding Tibet, Taiwan, Hong Kong, and Macau. The research time frame selected for analysis spans from 2010 to 2021. The specific indicators are derived from China City Statistical Yearbook (http://www.stats.gov.cn/sj/ndsj/), China Urban Construction Statistical Yearbook (https://www.mohurd.gov.cn/gongkai/fdzdgknr/sjfb/index.html), China Statistical Yearbook on Environment (http://www.stats.gov.cn/zs/tjwh/tjkw/tjzl/), Bulletin of Flood and Drought Disasters in China (http://www.mwr.gov.cn/sj/tjgb/zgshzhgb/), China Statistical Yearbook (http://www.stats.gov.cn/), and other sources. The meteorological data used mainly comes from the China Meteorological Administration (https://www.cma.gov.cn/). Due to the lack of data and inconsistent source dimensions, interpolation is used to supplement missing data.

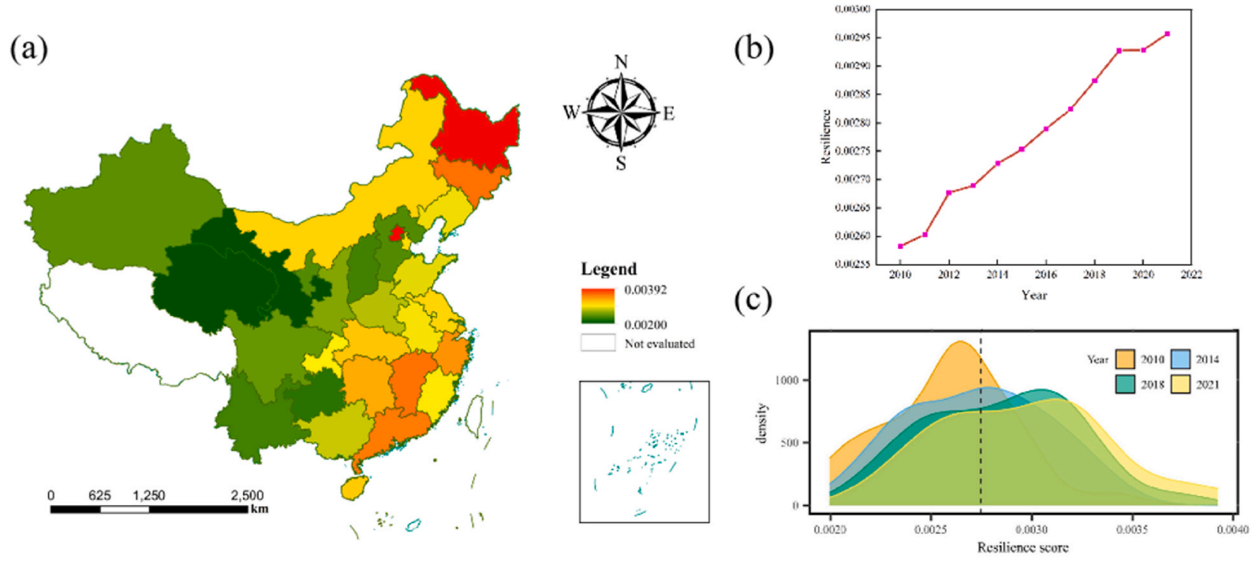

Fig. 3. Spatial-temporal distribution characteristics of drought resilience: (a) spatial distribution characteristics; (b) trend chart of drought resilience index; (c) distribution map of drought resilience density.

3. Results

3.1. Spatial-temporal heterogeneity of drought resilience

The average drought resilience score for the 30 provinces in China is 0.00278, indicating a moderate level of resilience (Fig. 3a). During the study period, eight provinces achieved an average drought resilience score above 0.003, namely Beijing, Heilongjiang, Jilin, Jiangxi, Guangdong, Hunan, Zhejiang, and Fujian. Two provinces, Gansu and Qinghai, had drought resilience scores below 0.0022. There are significant differences in drought resilience among different provinces, with Beijing, the province with the highest resilience, scoring 1.64 times higher than Qinghai, the province with the lowest resilience. From 2010 to 2021, China's drought resilience showed an upward trend (Fig. 3b). The average drought resilience index for China increased from 0.00258 in 2010 to 0.00296 in 2021, representing a 12.7 % improvement over the past 12 years. The rise was relatively fast in the first ten years, but the impact of the COVID-19 pandemic slowed progress in 2020. Notably, the differences in drought resilience among Chinese provinces have become smaller since 2010 (Fig. 3c). The analysis of density distribution charts shows the evolution from a unimodal to a bimodal distribution, indicating an overall upward trend in China's drought resilience. However, the improvement in resilience values remains limited as the curve shifts horizontally to the right with a decrease in peak values. Overall, China's drought resilience has improved to some extent with socioeconomic development, but further efforts are needed to enhance resilience across the nation.

This paper analyzed the spatial distribution of drought resilience and used the average of drought resilience natural breakpoints in 2010, 2015 and 2021 as our classification criteria (Table S3). Upon examining China's drought resilience capacity, one can discern a notable evolution in its capability over time (Fig. 4). In 2010, there were more provinces with low resilience, accounting for 26.7 %, mainly concentrated in western China. In 2010, Beijing was a region with relatively high overall resilience, while areas with higher resilience were primarily concentrated in southern China. Compared to 2010, the number of provinces with higher resilience in China significantly increased in 2014 and 2018, indicating a substantial improvement in overall resilience levels. The number of provinces with lower resilience levels has decreased, mainly concentrated in western China. The number of provinces with a high drought resilience level increased to 2 in 2014 and 4 in 2018, with these provinces mainly concentrated in the eastern and northeastern regions. In 2021, the overall drought resilience level was the highest, with 5 provinces classified as having high drought resilience level and 11 provinces as having relatively high drought resilience level. These provinces were primarily located in eastern and northeastern China.

Provinces in the eastern region of China manifest remarkable resilience (Table S4), especially in the southeastern areas, where

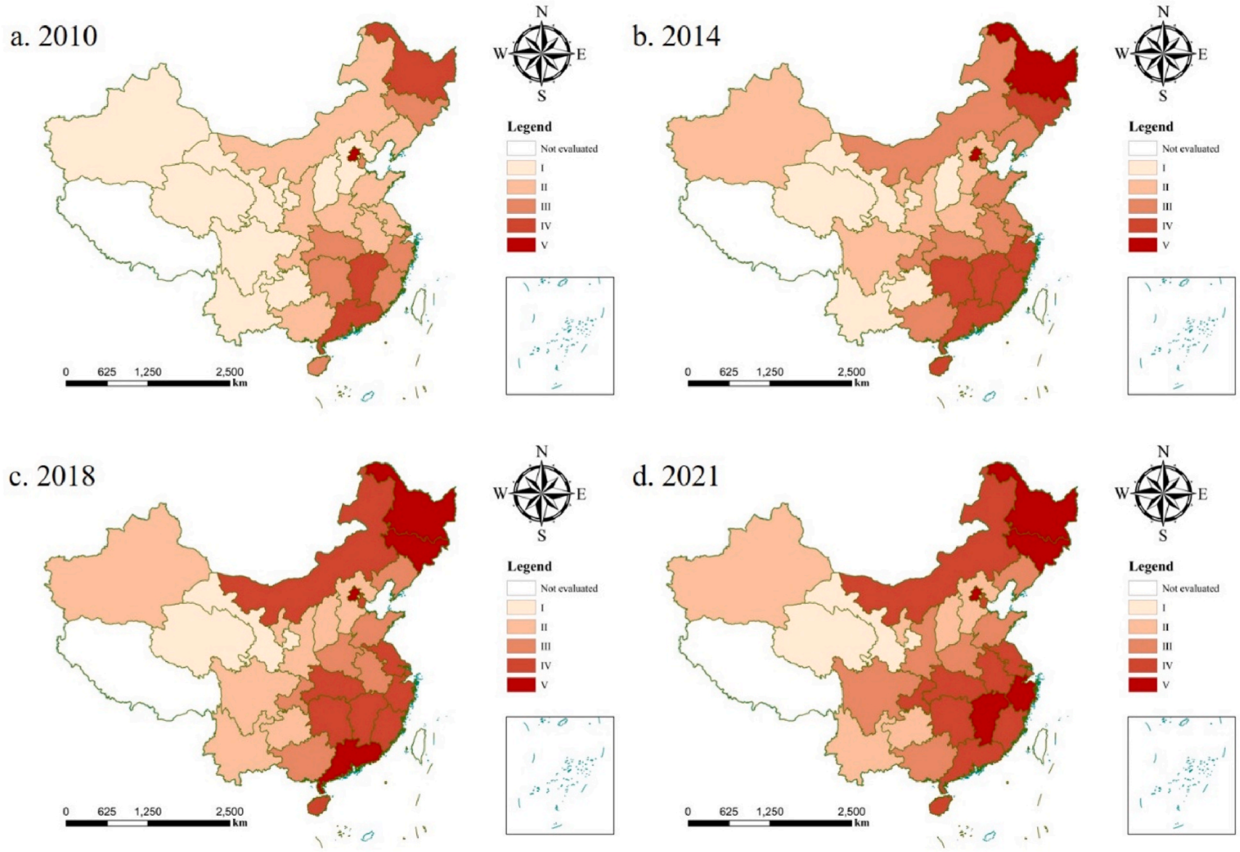

Fig. 4. Spatial distribution characteristics of drought resilience in China over time.

robust per capita GDP growth has endowed them with impressive post-disaster recovery capabilities. Additionally, their agricultural contribution to GDP and the proportion of the rural population are relatively modest. In contrast, the northeastern region, characterized by a sparse population and a high per capita grain yield, coupled with its higher latitude, cooler temperatures, and reduced evaporation, collectively enhances its resilience. In stark contrast, the western region, due to its limited precipitation and modest per capita GDP, along with a higher rural population proportion, exhibits lower drought resilience.

By further utilizing the weights of various drought resilience indicators, we can obtain scores for SR, EcoR, IR and EnvR in different regions of China (Fig. 5 and Table S5). The four major regions exhibit varying levels of performance in different sub-resilience categories. The eastern region leads in IR and SR. The central region demonstrates excellent performance in IR. The northeastern region excels in EcoR. Apart from the western region, which slightly lags behind, the other three regions show relatively similar levels of EnvR. This indicates that each of the four major regions in China has its own strengths and weaknesses in different aspects of resilience. The eastern region has a strong institutional and SR, while the central region shows remarkable performance in IR. The northeastern region excels in EcoR.

The overall difference in drought resilience among provinces in China has widened over the years (Fig. 6), with the overall Theil index increasing from 0.0076 in 2010 to 0.0095 in 2019, slightly declining, and then rising again to 0.0095 (Table S6). Between 2010 and 2021, variations in China's drought resilience were predominantly attributable to intra-regional disparities, contributing to 90 % of the overall differentiation. This fluctuated, initially decreasing and subsequently increasing, with the contribution rate consistently exceeding 90 %. Inter-group variances showed a general trend of initial growth followed by a decline in their contribution to the overall disparity. This indicates that the overarching differential in China's drought resilience is primarily a consequence of intra-regional variations. Examining the Theil Index across the four major economic regions reveals that from 2010 to 2021, the north-east saw a notable escalation in its Theil Index and its contribution rate. This rose from 8 % in 2010 to 23.9 % by 2021. The Theil Indices for the remaining regions oscillated, with the western region maintaining a generally elevated Theil Index and consistently contributing approximately 40 % to the overall disparity, the highest among the four regions. Both the eastern and central regions

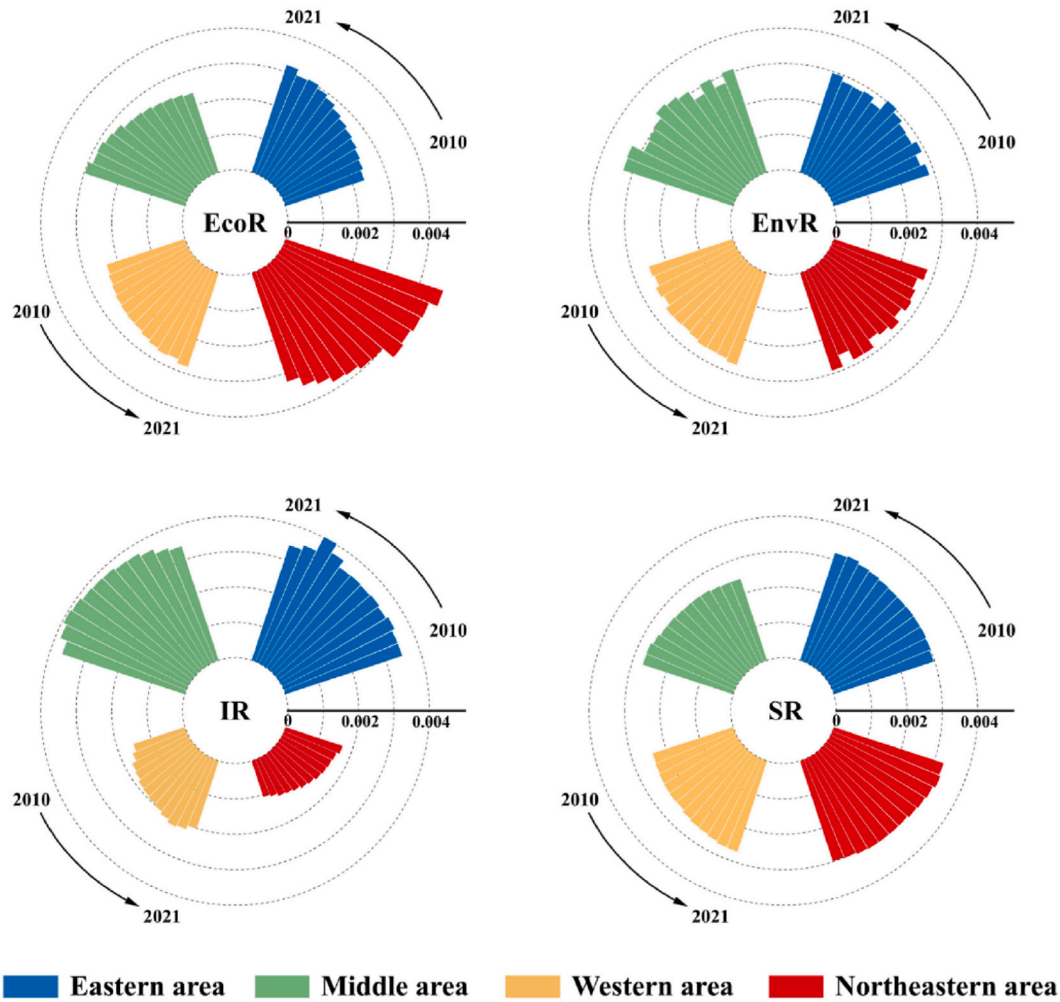

Fig. 5. Sub-resilience levels of China's four major regions.

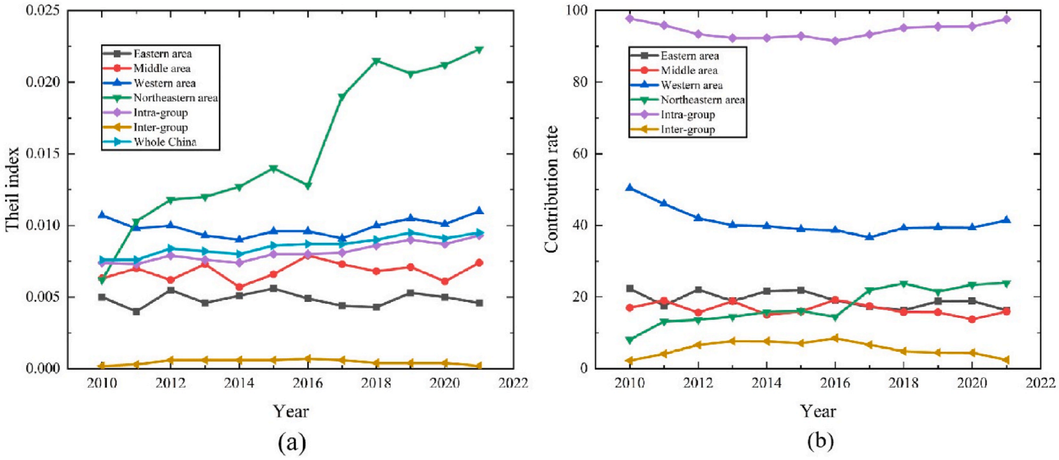

Fig. 6. Regional differences of drought resilience: (a) change trend of Theil index; (b) change trend of contribution rate.

witnessed a cyclical decline in their contribution rates, albeit with a lesser magnitude than the western region. This suggests that in future endeavors to harmonize drought resilience development across regions, the western region should be prioritized.

3.2. Dependence and hotspot detection of drought resilience

As shown in Table 2, from 2010 to 2021, Moran's I value range from 0.372 to 0.522, with p-values below 0.001 and Z-scores surpassing 3.38, indicating strong spatial autocorrelation. The estimates reveal two trends: an increase from 0.372 in 2010 to 0.522 in 2016, with significant growth in the initial three years, followed by a gradual decline to 0.46 by 2021. These changes suggest a high-high or low-low spatial clustering phenomenon, where provinces with high drought resilience are surrounded by similar provinces, and vice versa. The upward trend from 2010 to 2016 indicates improved resilience with China's socioeconomic progress. Consequently, the clustering degree of regions also increases. The overall Moran's I index decreased from 0.522 in 2016 to 0.46 in 2021, suggesting an increased number of provinces with high drought resilience and overall favorable development. Provinces show a tendency towards spatial diffusion, and the spatial clustering degree slightly decreases.

The Moran's I serves as a crucial indicator to assess the spatial dependency of China's Drought Resilience Index. From 2010 to 2021, all Chinese provinces exhibited a global spatial autocorrelation in their drought resilience. To identify hotspots and coldspots of drought resilience, the Getis-Ord Gi* method was employed, illustrating the clustering pattern across provinces during this period (Fig. 7).

The analysis detected low-value clusters in the northwest and southwest regions, while high-value clusters were identified in the southeast and northeast regions. The number of provinces with high-value clusters has changed from year to year, increasing from three in 2010 to five in 2014 and decreasing to three in 2021. Conversely, the number of low-value clusters remained constant throughout the study. Spatial correlation revealed that the northeast region initially lacked high-value clusters, but by 2014, Heilongjiang and Jilin became hotspot areas, with Heilongjiang as the primary hotspot. In the southeast region, the hotspot range fluctuated, with only Jiangxi consistently identified as a high-value cluster, though its correlation with neighboring provinces decreased. The low-value correlation in the western region experienced an initial increase followed by a decrease. Qinghai and Sichuan remained primary coldspot areas throughout the study period, while the low-value correlation in other provinces fluctuated.

Considering the changing characteristics of coldspot and hotspot distribution locations and ranges, the focus of drought resilience

Table 2
Global Moran index of drought resilience.

Year	Moran's I	p-value	z-value
2010	0.372	0.001	3.3805
2011	0.489	0.001	3.9661
2012	0.504	0.001	4.2417
2013	0.506	0.001	4.0575
2014	0.506	0.001	4.0682
2015	0.511	0.001	4.1145
2016	0.522	0.001	4.1987
2017	0.495	0.001	4.0178
2018	0.493	0.001	4.0013
2019	0.476	0.001	3.8583
2020	0.476	0.001	3.9043
2021	0.460	0.001	3.8425

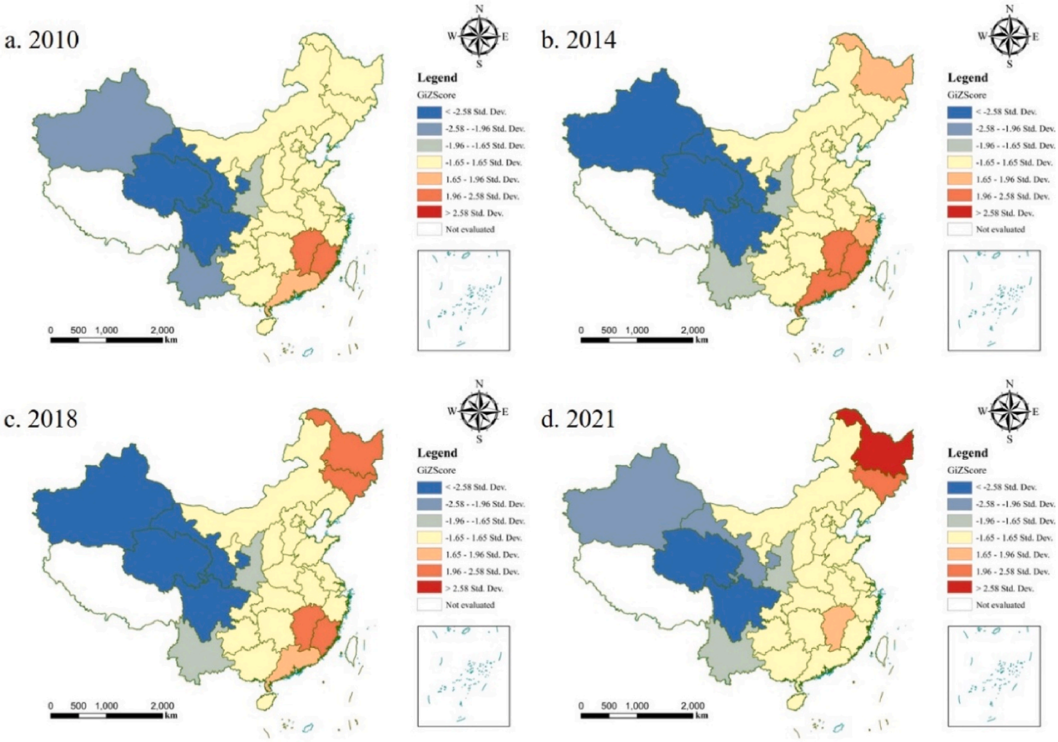

Fig. 7. Cold and hot spots pattern of drought resilience.

research during the study period should be on the western region. Additionally, attention should be paid to the rapid decline in high-value correlation in the southeast region in recent years.

3.3. The impact mechanism of drought resilience

In this study, we employed SEM to analyze the impact of various sub-resilience factors on overall drought resilience in China. Specifically, the model included some manifest variables representing the latent constructs of economic, social, environmental, and institutional resilience. The manifest variables for economic resilience (EcoR) included the proportion of agriculture in GDP (X1) and GDP per capita (X2), reflecting the region's economic capacity to withstand and recover from drought. For social resilience (SR), variables such as population density (X18) and the proportion of urban residents enrolled in social insurance (X16) were used, indicating the social infrastructure's ability to support affected populations. Environmental resilience (EnvR) was measured using

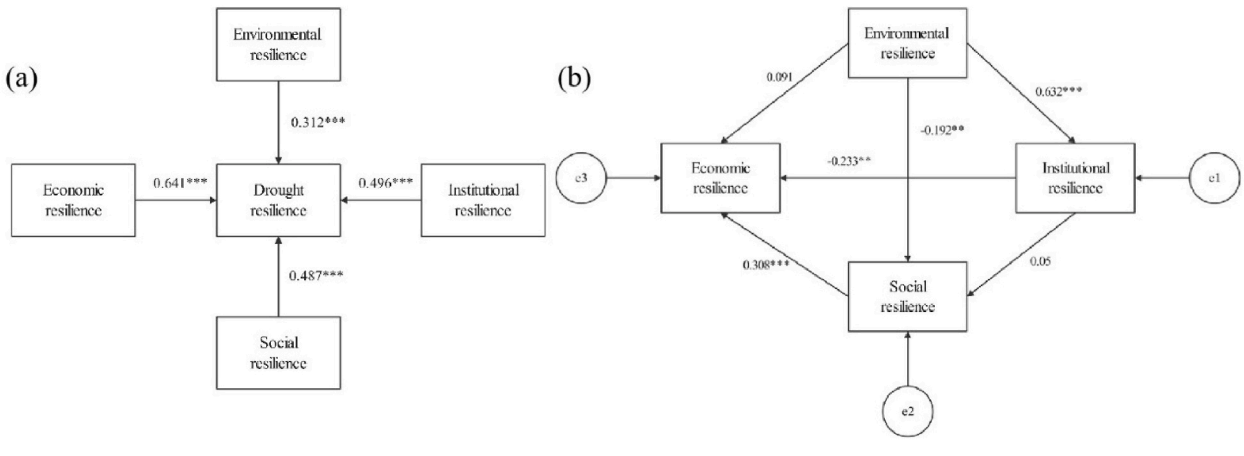

Fig. 8. The results of SEM model: (a) Interaction between drought resilience and sub-domain resilience; (b) Interaction within sub-domain resilience (**p < 0.01, ***p < 0.001).

indicators like forest coverage (X6) and average annual precipitation (X8), while institutional resilience (IR) was captured through variables such as effective irrigation rate (X13) and sewage treatment rate (X15). These manifest variables were critical in assessing the multidimensional nature of drought resilience, and their inclusion in the SEM allowed for a more nuanced understanding of the interactions between sub-resilience factors and overall drought resilience. The model results for drought resilience and sub-resilience are depicted in Fig. 8. To clearly illustrate the path relationships, we have removed insignificant paths to emphasize the relationships between drought resilience and the four sub-resilience factors.

The measurement results indicate that all sub-resilience factors have a positive influence on drought resilience. The path coefficients for EcoR, EnvR, IR, and SR on drought resilience are 0.641, 0.312, 0.496, and 0.487, respectively. Based on the analysis, all four paths between Chinese drought resilience and sub-resilience are significant at the level of $p < 0.001$, reflecting the positive and significant impacts of the sub-resilience factors on drought resilience. The structural equation model depicting the interactions among the sub-resilience factors is presented in Fig. 8. Since this model is a saturated model, meaning that all the parameters to be estimated are exactly equal to the elements in the covariance matrix, the degrees of freedom are zero. Therefore, fit indices are not estimated for this model, and we solely focus on the path coefficients.

There are a total of six paths in the model, with four of them reaching a significance level of 0.05. Specifically, EnvR has a direct influence on IR and SR, with standardized path coefficients of 0.632 and −0.192. SR and IR have a direct influence on EcoR, with standardized path coefficients of 0.308 and −0.233. Based on the interactions within the sub-resilience factors, IR and SR mediate the effects of economic and EnvR. The total effects of each sub-resilience factor on drought resilience are illustrated in Fig. 9. Drought resilience is predominantly influenced by SR and EcoR, with values of 0.684 and 0.641 respectively. Following this is IR with a total effect of 0.3467. Although IR is not as pronounced as its SR and EcoR, its presence underscores the imperative of clear, transparent, and efficient policy and management strategies to ensure optimal resource allocation and utilization. While EnvR exhibits the least effect at 0.18, it serves as a poignant reminder of the enduring significance of environmental conservation.

3.4. Dynamic simulation of drought resilience

As shown in Fig. 10, the drought resilience level in China generally shows an upwards trend from 2022 to 2035. Among them, the years 2022–2026 showcase a diminishing resilience trend attributed to the disruptive impact of the COVID-19 pandemic. The resultant vulnerabilities ripple across various aspects, contributing to the observed downturn. However, from 2026 to 2035, as the pandemic's effects wane, there is a notable resurgence in drought resilience. This period witnesses a strengthening of resilience and growth as adverse pandemic-related effects recede.

Throughout the forecast period, a majority of Chinese provinces are categorized under Level I and Level II resilience tiers. Notably, western regions grapple with lower resilience, particularly in the initial stages. Yet, provinces such as Yunnan, Gansu, and Sichuan in the western sector exhibit remarkable progress, possibly influenced by higher inherent resilience in central areas and reduced pandemic impact. In contrast, drought resilience in the eastern regions remains relatively steady, marked by minor fluctuations. In essence, China's overall drought resilience continues to be influenced by the lingering effects of the pandemic, resulting in a relatively modest level of resilience. Amongst the geographical divisions, the western region stands out with the lowest resilience, while the northeastern region boasts consistently high average resilience. Heilongjiang in the northeast maintains a remarkable Level V resilience. The central and eastern regions remain basically unchanged, with select provinces noting slight enhancements and others witnessing marginal declines.

In this study, regarding drought resilience levels prediction, the BP neural network model demonstrated exceptional performance (Table S7). The model achieved an Average Root Mean Square Error (RMSE) of 0.0593, indicating minimal differences between the predicted and actual values. Additionally, Average R-squared (R^2) value of the model was 0.9056, underscoring a strong correlation between the predicted and observed outcomes. The model consistently exhibited strong fitting capabilities across different training and testing sets. In conclusion, the BP neural network model used in this study shows high accuracy and reliability in predicting drought resilience levels.

Further, a 3D map of the predicted drought resilience levels from 2022 to 2035 was generated in this study using the trend analysis

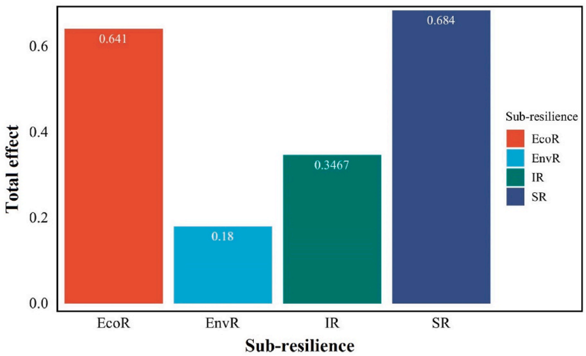

Fig. 9. The total effect of sub-resilience on drought resilience.

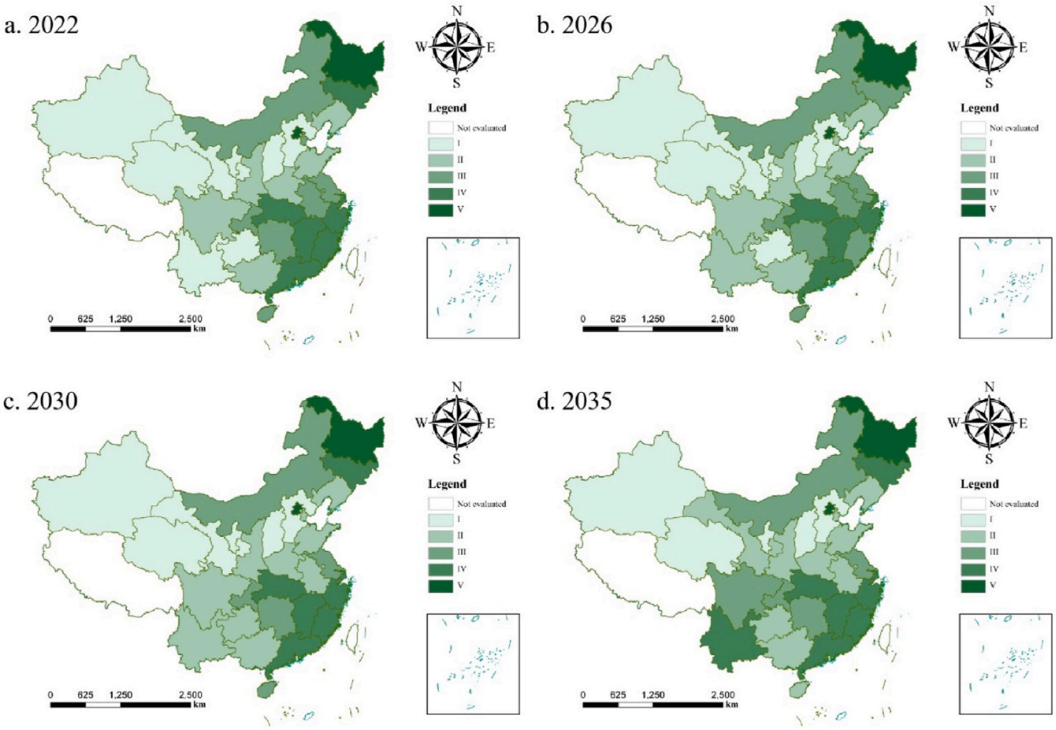

Fig. 10. Dynamic simulation results of drought resilience level from 2022 to 2035.

tool in ArcGIS 10.5. Visualized as scatter plots projected onto the X-Y plane (longitude and latitude) with varying heights (Z-axis), Fig. 11 underscores the divergence in drought resilience between the east-west and north-south orientations. In 2022 reflects an "east high, west low" pattern, as drought resilience incrementally ascends from west to east. Conversely, the north-south dimension follows a "U" shape, signifying a decline succeeded by a recovery from south to north. This configuration underscores higher drought resilience in the eastern provinces relative to their western counterparts, and collectively, the southern and northern provinces exhibit greater resilience levels compared to the central provinces. From 2026 to 2035, the north-south trend retains stability with minimal shifts. However, the east-west trajectory gradually decelerates, indicating a sustained improvement in drought resilience across western provinces, alongside a slight dip in the average resilience within the eastern provinces.

4. Discussion

Amid the escalating dynamics of global climate change, the future water cycle and hydrological processes are undergoing transformation [55]. Numerous climatic models prognosticate a potential intensification in both the frequency and severity of drought events in forthcoming years [56–58]. For China, this shifting climatic paradigm poses a direct impediment to its sustainable progression [59,60]. As the most populous nation globally, several regions within China are already grappling with water scarcity challenges. Droughts exert immense strain on agriculture, industries, and public water supplies in China, inflicting significant socio-economic repercussions. Contemporary studies denote that meteorological droughts are predominantly observed in North and Southwest China, with heightened vulnerability concentrated in the Northwest, North, and Southwest regions [61–65]. These findings align congruently with the conclusions of the present study [66,67]. Moreover, comparing the results of this study with previous research findings, the data analysis results align well with the research outcomes of other regions in China, indicating that the current data measurements in this study are more reliable [64,65,68]. This study indicates that the drought resilience level in China shows an upwards trend, but there are significant regional differences among the provinces, which is consistent with the conclusion of the previous research findings [67,69]. When comparing the differences in sub-resilience levels among regions, it is evident that there are significant variations in EcoR and IR levels among the four major regions. EnvR is predominantly influenced by geographical location, and research has identified an enhanced recovery capability of ecosystems from arid zones to semi-humid regions against droughts [70]. Regions can bolster their drought resilience through afforestation initiatives and by moderating grazing intensities [71]. Moreover, this study reveals that in regions subjected to drought-induced environmental stressors, a robust social network and a sturdy economic framework could potentially offer greater support and adaptive capacity to individuals [72,73]. Regions in the Northwest, such as Qinghai and Gansu, consistently exhibit subpar drought resilience. Beyond meteorological and environmental determinants, the pronounced institutional vulnerability in Qinghai and Gansu stands out as a pivotal contributor to their diminished resilience. The limited capacity of small reservoirs in Qinghai and Gansu impedes prompt resource allocation during droughts. There's an imperative

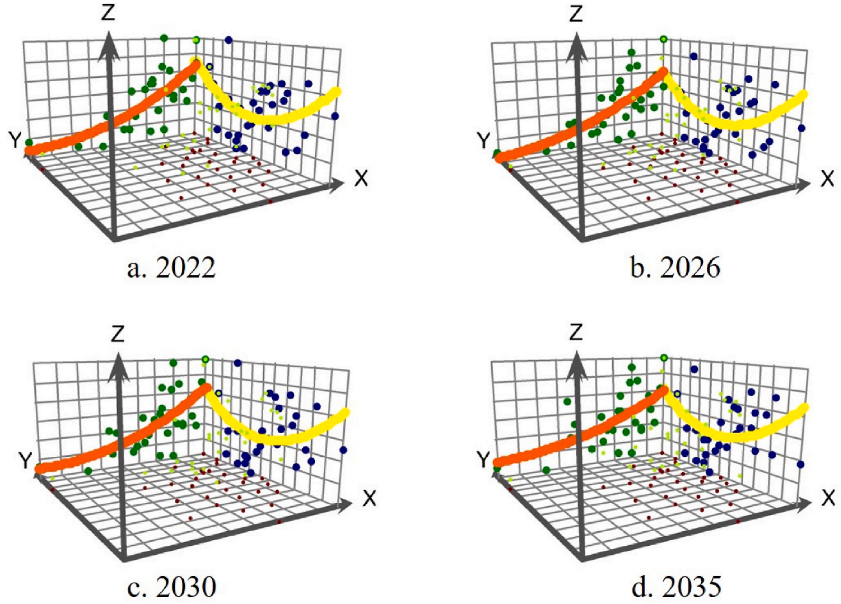

Fig. 11. Trend lines of China's drought resilience levels.

to recognize the significance of establishing small reservoirs from an institutional standpoint, fostering an extensive network of such infrastructures [74]. Additionally, Gansu's per capita GDP lingers at merely 50 % of the national average, exacerbating its resilience deficit. During the pandemic, the socio-economic fabric of the Eastern coastal regions suffered, leading to a pronounced dip in drought resilience. Establishing preventive mechanisms to mitigate impacts on drought resilience during urban lockdowns becomes vital.

Enhancing drought resilience becomes paramount in the context of climate change. For China's regional sustainable development, amplifying drought resilience signifies an augmented capacity to confront climatic challenges, ensuring stable resource provisions and fostering favorable conditions for future advancement [75–78]. This study proposes the following policy recommendations for improving drought resilience in China.

Firstly, strengthen economic and technological support from eastern affluent regions to western provinces. Given the challenges in rapidly improving economic infrastructure in Western provinces, it is crucial for the more developed Eastern regions to increase their economic and technological investments in these areas. This includes funding infrastructure projects that can enhance the resilience of Western provinces, particularly in the face of natural disasters. Investments should be directed toward modernizing agricultural practices in Western provinces. This could involve introducing advanced irrigation systems, sustainable farming techniques, and agricultural technologies that improve productivity and resilience against droughts and other climate-related challenges [79,80]. The use of big data technologies, including satellite remote sensing, meteorological radar, and seismic monitoring systems, should be encouraged. These technologies can significantly improve data collection and sharing, facilitating timely and accurate disaster warnings and responses in the Western provinces.

Secondly, establish disaster monitoring platforms and increase public awareness. The establishment of disaster-monitoring platforms that aggregate crowd-sourced data is essential. These platforms can enable governmental agencies to accurately pinpoint affected areas during disasters and assess the severity of the impact, thereby improving response efforts. Public awareness campaigns on emergency management should be intensified to educate the populace about disaster preparedness. Encouraging proactive disaster monitoring and information-sharing among citizens can significantly enhance the overall resilience and recovery capabilities of communities [81].

Furthermore, accelerate the optimization of resource allocation to boost drought resilience. Targeted investments in infrastructure and ecological protection are necessary to enhance the drought resilience of Western provinces. These investments should prioritize projects that improve water management, soil conservation, and ecological restoration, thereby reducing the regions' vulnerability to drought [82,83]. The Central-South region, with its stronger technical and financial resources, should play a pivotal role in supporting Western provinces. This can be achieved by optimizing resource allocation and establishing inter-provincial collaboration mechanisms that facilitate resource sharing and mutual support.

Establish drought resilience research and technology centers in high-resilience provinces. High-resilience provinces, particularly in the central region, should establish drought resilience research and technology centers. These centers can provide technical expertise, develop innovative solutions, and offer policy recommendations to help other provinces enhance their drought resilience. Long-term planning is essential to address the complex interplay between pandemic impacts and drought resilience. These plans should include provisions for increased support to affected regions, ensuring that they have the capacity to withstand and recover from both droughts and pandemic-related disruptions [84,85].

Foster inter-provincial collaboration to enhance overall drought resilience. Collaboration among provinces, particularly between the Northeast, Central, and Eastern regions, should be strengthened. This can involve creating formal mechanisms for resource sharing, joint disaster response initiatives, and collaborative research efforts aimed at improving drought resilience across regions [86,87]. The implementation of sustainable development initiatives that focus on long-term resilience is crucial. By fostering cooperation and leveraging the strengths of different regions, China can enhance its overall ability to manage and mitigate drought risks, thereby supporting sustainable development in the face of evolving climate challenges.

5. Conclusion

In this study, we proposed a comprehensive framework to assess drought resilience based on "Social-Economic-Environmental-Institutional" dimensions in China, analyzing its spatiotemporal evolution characteristics, uncovering the underlying impact mechanisms, and projecting future resilience trends across different regions of the country. 30 provinces in China are used as the study area for research discussions and results analysis. The main conclusions are as follows.

(1) The overall level of drought resilience in China exhibited an upward trend from 2010 to 2021. The rate of improvement in drought resilience was relatively rapid during the first decade, but it slowed down due to the impact of the COVID-19 pandemic in 2020, resulting in no change in resilience that year. In 2021, there was a slight increase in drought resilience. From a spatial perspective, there is significant positive spatial autocorrelation in drought resilience across China, with high-value clusters emerging in the southeastern and northeastern regions. The central and eastern coastal provinces exhibit relatively high levels of drought resilience, while the western inland regions show lower resilience, indicating distinct regional disparities.
(2) All sub-resilience factors positively influence drought resilience. The path coefficients for EcoR, EnvR, IR, and SR on drought resilience are 0.641, 0.312, 0.496, and 0.487, respectively. Based on the interactions among sub-resilience factors, IR and SR mediate the impact of EcoR and EnvR. Drought resilience is primarily influenced by SR and EcoR, followed by IR, with EnvR showing the least impact.
(3) The level of drought resilience in China is projected to continue its upward trend from 2022 to 2035. However, in the early years, the improvement in drought resilience across provinces is expected to be slow due to the lingering effects of the pandemic. The western region will continue to have the lowest drought resilience, although provinces like Yunnan, Gansu, and Sichuan in the west are expected to show significant improvement. The eastern region is expected to maintain relatively stable levels of drought resilience. In terms of spatial development trends, significant differences in drought resilience are evident in both the east-west and north-south directions, with a general pattern of "higher in the east and lower in the west." In the later years, the north-south differences are expected to remain stable, with minimal changes.

This research aims to identify the resilience and spatial variations of Chinese provincial-level administrative regions concerning drought. The findings shed light on regions in China that currently and in the future require attention regarding drought resilience, emphasizing the significance of social and institutional systems in enhancing drought resilience. These issues not only concern China but also affect the sustainable development of all countries worldwide. A deeper understanding of regional drought resilience is crucial for safeguarding precious water resources, optimizing ecosystems, and providing scientific guidance for sustainable agricultural and socio-economic development. Only through in-depth research into drought resilience can we better confront the threat of drought posed by climate change, thus ensuring societal safety and economic sustainability.

Data availability statement

Data included in article/supp. material/referenced in article.

CRediT authorship contribution statement

Huihui Wang: Writing – review & editing, Writing – original draft, Methodology, Investigation, Funding acquisition, Formal analysis, Data curation, Conceptualization. **Xiaoyong Gao:** Writing – original draft, Methodology, Investigation, Formal analysis, Data curation. **Yunsong Yang:** Data curation. **Zhengzao Wang:** Methodology, Data curation. **Shuhong You:** Data curation. **Hanyu Xue:** Data curation. **Wanlin He:** Data curation.

Declaration of competing interest

The authors declare that they have no known competing financial interests or personal relationships that could have appeared to influence the work reported in this paper.

Acknowledgement

This work was supported by National Natural Science Foundation of China (No. 42201241), and National Key Research and Development Project of China (No. 2021YFC3101700). The authors would like to thank the anonymous reviewers for their helpful and constructive comments.

Appendix A. Supplementary data

Supplementary data to this article can be found online at https://doi.org/10.1016/j.heliyon.2024.e38533.

References

[1] H. Cooley, K. Donnelly, R. Phurisamban, M. Subramanian, Impacts of California's Ongoing Drought: Agriculture, Pacific Institute, Oakland, CA, USA, 2015.
[2] P.U. Rasmussen, A.E. Bennett, A.J. Tack, The impact of elevated temperature and drought on the ecology and evolution of plant-soil microbe interactions, J. Ecol. 108 (1) (2020) 337–352.
[3] Y. Ding, M.J. Hayes, M. Widhalm, Measuring economic impacts of drought: a review and discussion, Disaster Prev. Manag. 20 (4) (2011) 434–446.
[4] T.R. Ault, On the essentials of drought in a changing climate, Science 368 (6488) (2020) 256–260.
[5] Z. Zhu, W. Duan, S. Zou, Z. Zeng, Y. Chen, M. Feng, J. Qin, Y. Liu, Spatiotemporal characteristics of meteorological drought events in 34 major global river basins during 1901–2021, Sci. Total Environ. 921 (2024) 170913.
[6] A.B. Smith, R.W. Katz, US billion-dollar weather and climate disasters: data sources, trends, accuracy and biases, Nat. Hazards 67 (2) (2013) 387–410.
[7] H. Guo, J. Chen, C. Pan, Assessment on agricultural drought vulnerability and spatial heterogeneity study in China, Int. J. Environ. Res. Publ. Health 18 (9) (2021) 4449.
[8] BFDDC, Bulletin of flood and drought disasters in China), Ministry of Water Resources the People's Republic of China: China, 2019, http://www.mwr.gov.cn/sj/tjgb/zgshzhgb/, 2019.
[9] G. Cai, S. Chen, Y. Liu, H. Sun, C. Chen, D. Gui, D. Yan, Using multiple indexes to analyze temporal and spatial patterns of precipitation and drought in Xinjiang, China, Theor. Appl. Climatol. 142 (2020) 177–190.
[10] M. Hagenlocher, I. Meza, C.C. Anderson, A. Min, F.G. Renaud, Y. Walz, Z. Sebesvari, Drought vulnerability and risk assessments: state of the art, persistent gaps, and research agenda, Environ. Res. Lett. 14 (8) (2019) 083002.
[11] J. Birkmann, O.D. Cardona, M.L. Carreño, A.H. Barbat, M. Pelling, S. Schneiderbauer, T. Welle, Framing vulnerability, risk and societal responses: the MOVE framework, Nat. Hazards 67 (2013) 193–211.
[12] G.C. Gallopín, Linkages between vulnerability, resilience, and adaptive capacity, Global Environ. Change 16 (3) (2006) 293–303.
[13] Y. Lei, J.A. Wang, Y. Yue, H. Zhou, W. Yin, Rethinking the relationships of vulnerability, resilience, and adaptation from a disaster risk perspective, Nat. Hazards 70 (2014) 609–627.
[14] A. Fekete, G. Hufschmidt, S. Kruse, Benefits and challenges of resilience and vulnerability for disaster risk management, International journal of disaster risk science 5 (2014) 3–20.
[15] P.J.G. Ribeiro, L.A.P.J. Gonçalves, Urban resilience: a conceptual framework, Sustain. Cities Soc. 50 (2019) 101625.
[16] T.L. Du, D.D. Bui, J. Buurman, X.T. Quach, Towards adaptive governance for urban drought resilience: the case of Da Nang, Vietnam, Int. J. Water Resour. Dev. 34 (4) (2018) 597–615.
[17] P. Aldunce, R. Bórquez, C. Adler, G. Blanco, R. Garreaud, Unpacking resilience for adaptation: incorporating practitioners' experiences through a transdisciplinary approach to the case of drought in Chile, Sustainability 8 (9) (2016) 905.
[18] T.L.T. Du, D.D. Bui, M.D. Nguyen, H. Lee, Satellite-based, multi-indices for evaluation of agricultural droughts in a highly dynamic tropical catchment, Central Vietnam, Water 10 (5) (2018) 659.
[19] X. Zhang, N. Chen, H. Sheng, C. Ip, L. Yang, Y. Chen, D. Niyogi, Urban drought challenge to 2030 sustainable development goals, Sci. Total Environ. 693 (2019) 133536.
[20] N.P. Simpson, K.J. Simpson, C.D. Shearing, L.R. Cirolia, Municipal finance and resilience lessons for urban infrastructure management: a case study from the Cape Town drought, Int. J. Urban Sustain. Dev. 11 (3) (2019) 257–276.
[21] B.W. Head, Managing urban water crises: adaptive policy responses to drought and flood in Southeast Queensland, Australia, Ecol. Soc. 19 (2) (2014).
[22] N.Q. Vinh, N.T. Khanh, P.T. Anh, The inter-relationships between lst, ndvi, ndbi in remote sensing to achieve drought resilience in ninh thuan, vietnam, in: ICSCEA 2019: Proceedings of the International Conference on Sustainable Civil Engineering and Architecture, Springer, Singapore, 2020, pp. 201–209.
[23] J. Cai, M. Kummu, V. Niva, J.H. Guillaume, O. Varis, Exposure and resilience of China's cities to floods and droughts: a double-edged sword, Int. J. Water Resour. Dev. 34 (4) (2018) 547–565.
[24] C.L. Hwang, A.S.M. Masud, Multiple Objective Decision Making-Methods and Applications: a State-Of-The-Art Survey, vol. 164, Springer Science & Business Media, 2012.
[25] P.F. Hsu, M.G. Hsu, Optimizing the information outsourcing practices of primary care medical organizations using entropy and TOPSIS, Qual. Quantity 42 (2008) 181–201.
[26] S.A. Jozi, M. Shafiee, N. MoradiMajd, S. Saffarian, An integrated Shannon's Entropy–TOPSIS methodology for environmental risk assessment of Helleh protected area in Iran, Environ. Monit. Assess. 184 (2012) 6913–6922.
[27] S. Kingir, A. Karakas, A. Öztel, Evaluation of university employees' work behaviours performance via entropy based TOPSIS methods, Elektronik Sosyal Bilimler Dergisi 15 (58) (2016) 1046–1058.
[28] X. Li, X. Meng, X. Ji, J. Zhou, C. Pan, N. Gao, Zoning technology for the management of ecological and clean small-watersheds via *k*-means clustering and entropy-weighted TOPSIS: a case study in Beijing, J. Clean. Prod. 397 (2023) 1–10.
[29] L. Anselin, Local indicators of spatial association-LISA, Geogr. Anal. 27 (2) (1995) 93–115.
[30] W. Musakwa, A. Van Niekerk, Monitoring urban sprawl and sustainable urban development using the Moran Index: a case study of Stellenbosch, South Africa, Int. J. Appl. Geospatial Res. (IJAGR) 5 (3) (2014) 1–20.
[31] L. Anselin, I. Syabri, Y. Kho, GeoDa: an introduction to spatial data analysis.", in: Handbook of Applied Spatial Analysis: Software Tools, Methods and Applications, Springer Berlin Heidelberg, Berlin, Heidelberg, 2009, pp. 73–89.
[32] J.K. Ord, A. Getis, Local spatial autocorrelation statistics: distributional issues and an application, Geographical analysis 27 (4) (1995) 286–306.
[33] M.S. Alam, N.J. Tabassum, Spatial pattern identification and crash severity analysis of road traffic crash hot spots in Ohio, Heliyon 9 (5) (2023) 11053.
[34] S. Yan, H. Chen, Q. Quan, J. Liu, Evolution and coupled matching of ecosystem service supply and demand at different spatial scales in the Shandong Peninsula urban agglomeration, China, Ecol. Indicat. 155 (2023) 111052.
[35] D. Zhang, X. Xie, C. Zhou, Spatial influence of exposure to green spaces on the climate comfort of urban habitats in China, Urban Clim. 51 (2023) 101657.
[36] U.R. Manepalli, G.H. Bham, S. Kandada, Evaluation of hotspots identification using kernel density estimation (K) and Getis-Ord (Gi*) on I-630, in: 3rd International Conference on Road Safety and Simulation, vol. 21, National Academy of Sciences, 2011, pp. 14–16.
[37] Y. Cui, S.U. Khan, J. Sauer, M. Zhao, Exploring the spatiotemporal heterogeneity and influencing factors of agricultural carbon footprint and carbon footprint intensity: embodying carbon sink effect, Sci. Total Environ. 846 (2022) 157507.
[38] L. Chen, S. Liu, W. Cai, R. Chen, J. Zhang, Y. Yu, Carbon inequality in residential buildings: evidence from 321 Chinese cities, Environ. Impact Assess. Rev. 105 (2024) 107402.
[39] L.H. Cheng, H.M. Guo, Study on factors influencing coal mine work safety based on SEM, China Saf. Sci. J. 28 (1) (2018) 137–142.
[40] J. Xu, Z. Li, H. Wang, Y. Zhang, X. Zhang, Construction safety influencing factor analysis of bridge-erecting machines based on structural equation modeling, Heliyon 10 (2) (2024) 101153.

[41] L. Klem, Structural equation modeling, in: L.G. Grimm, P.R. Yarnold (Eds.), Reading and Understanding MORE Multivariate Statistics, American Psychological Association, 2000, pp. 227–260.
[42] P.W. Lei, Q. Wu, Introduction to structural equation modeling: issues and practical considerations, Educ. Meas. 26 (3) (2007) 33–43.
[43] A. Arlinghaus, D.A. Lombardi, J.L. Willetts, S. Folkard, D.C. Christiani, A structural equation modeling approach to fatigue-related risk factors for occupational injury, American journal of epidemiology 176 (7) (2012) 597–607.
[44] J.L. Zhou, B. Zhe-Hua, Z.Y. Sun, Safety assessment of high-risk operations in hydroelectric-project based on accidents analysis, SEM, and ANP, Math. Probl Eng. 2013 (1) (2013) 530198.
[45] G.T. Belay, B.H. Woldegiorgis, Y.T. Prasetyo, Structural equation modeling approach for the analysis of ergonomics risk factors and occupational injuries among building construction workers in Bahir Dar City-Ethiopia, Heliyon 10 (11) (2024) 530199.
[46] J. Li, J.H. Cheng, J.Y. Shi, F. Huang, Brief introduction of back propagation (BP) neural network algorithm and its improvement, in: Advances in Computer Science and Information Engineering, vol. 2, Springer Berlin Heidelberg, 2012, pp. 553–558.
[47] Y. Han, L. Cao, Z. Geng, W. Ping, X. Zuo, J. Fan, G. Lu, Novel economy and carbon emissions prediction model of different countries or regions in the world for energy optimization using improved residual neural network, Sci. Total Environ. 860 (2023) 160410.
[48] J. Chen, Z. Liu, Z. Yin, X. Liu, X. Li, L. Yin, W. Zheng, Predict the effect of meteorological factors on haze using BP neural network, Urban Clim. 51 (2023) 101630.
[49] A. Paszke, S. Gross, F. Massa, A. Lerer, J. Bradbury, G. Chanan, S. Chintala, Pytorch: an imperative style, high-performance deep learning library, Adv. Neural Inf. Process. Syst. 32 (2019).
[50] W. McKinney, Data structures for statistical computing in Python. Proceedings of the 9th Python in Science Conference, 2010, pp. 56–61.
[51] M. Stone, Cross-validatory choice and assessment of statistical predictions, J. Roy. Stat. Soc. B 36 (2) (1974) 111–133.
[52] H. Wang, W. He, Z. Zhang, X. Liu, Y. Yang, H. Xue, X. Gao, Spatio-temporal evolution mechanism and dynamic simulation of nitrogen and phosphorus pollution of the Yangtze River Economic Belt in China, Environmental Pollution (2024) 124402.
[53] D. Krstajic, L.J. Buturovic, D.E. Leahy, S. Thomas, Cross-validation pitfalls when selecting and assessing regression and classification models, J. Cheminf. 6 (2014) 1–15.
[54] S. Bates, T. Hastie, R. Tibshirani, Cross-validation: what does it estimate and how well does it do it? J. Am. Stat. Assoc. (2023) 1–12.
[55] J.B. Kim, J.M. So, D.H. Bae, Global warming impacts on severe drought characteristics in Asia monsoon region, Water 12 (5) (2020) 1360.
[56] L. Xu, N. Chen, X. Zhang, Global drought trends under 1.5 and 2 C warming, Int. J. Climatol. 39 (4) (2019) 2375–2385.
[57] M. Beniston, D.B. Stephenson, O.B. Christensen, C.A. Ferro, C. Frei, S. Goyette, K. Woth, Future extreme events in European climate: an exploration of regional climate model projections, Climatic Change 81 (2007) 71–95.
[58] G. Nikulin*, E. KjellströM, U. Hansson, G. Strandberg, A. Ullerstig, Evaluation and future projections of temperature, precipitation and wind extremes over Europe in an ensemble of regional climate simulations, Tellus Dyn. Meteorol. Oceanogr. 63 (1) (2011) 41–55.
[59] Y. Ding, S. Peng, Spatiotemporal trends and attribution of drought across China from 1901-2100, Sustainability 12 (2) (2020) 477.
[60] S.Y. Li, L.J. Miao, Z.H. Jiang, G.J. Wang, K.R. Gnyawali, J. Zhang, C. Li, Projected drought conditions in Northwest China with CMIP6 models under combined SSPs and RCPs for 2015-2099, Adv. Clim. Change Res. 11 (3) (2020) 210–217.
[61] H. Chang, G. He, Q. Wang, H. Li, J. Zhai, Y. Dong, J. Zhao, Use of sustainability index and cellular automata-Markov model to determine and predict long-term spatio-temporal variation of drought in China, J. Hydrol. 598 (2021) 126248.
[62] J. Chou, T. Xian, R. Zhao, Y. Xu, F. Yang, M. Sun, Drought risk assessment and estimation in vulnerable eco-regions of China: under the background of climate change, Sustainability 11 (16) (2019) 4463.
[63] L. Han, Q. Zhang, P. Ma, J. Jia, J. Wang, The spatial distribution characteristics of a comprehensive drought risk index in southwestern China and underlying causes, Theor. Appl. Climatol. 124 (2016) 517–528.
[64] P. Wang, W. Qiao, Y. Wang, S. Cao, Y. Zhang, Urban drought vulnerability assessment-A framework to integrate socio-economic, physical, and policy index in a vulnerability contribution analysis, Sustain. Cities Soc. 54 (2020) 102004.
[65] J. Zhao, Q. Zhang, X. Zhu, Z. Shen, H. Yu, Drought risk assessment in China: evaluation framework and influencing factors, Geography and Sustainability 1 (3) (2020) 220–228.
[66] Q. Wang, Y.Y. Liu, Y.Z. Zhang, L.J. Tong, X. Li, J.L. Li, Z. Sun, Assessment of spatial agglomeration of agricultural drought disaster in China from 1978 to 2016, Sci. Rep. 9 (1) (2019) 14393.
[67] D. Wu, D.H. Yan, G.Y. Yang, X.G. Wang, W.H. Xiao, H.T. Zhang, Assessment on agricultural drought vulnerability in the Yellow River basin based on a fuzzy clustering iterative model, Nat. Hazards 67 (2013) 919–936.
[68] S. Sun, Z. Wang, C. Hu, G. Gao, Understanding climate hazard patterns and urban adaptation measures in China, Sustainability 13 (24) (2021) 13886.
[69] H. Wang, X. Gao, T. Xu, H. Xue, W. He, Spatial-temporal evolution mechanism and efficiency evaluation of drought resilience system in China, J. Clean. Prod. 428 (2023) 139298.
[70] Y. Yao, B. Fu, Y. Liu, Y. Li, S. Wang, T. Zhan, D. Gao, Evaluation of ecosystem resilience to drought based on drought intensity and recovery time, Agric. For. Meteorol. 314 (2022) 108809.
[71] J.C. Ruppert, K. Harmoney, Z. Henkin, H.A. Snyman, M. Sternberg, W. Willms, A. Linstädter, Quantifying drylands' drought resistance and recovery: the importance of drought intensity, dominant life history and grazing regime, Global Change Biol. 21 (3) (2015) 1258–1270.
[72] S.A. Khatibi, A. Golkarian, A. Mosaedi, H. Sojasi Qeidari, Assessment of resilience to drought of rural communities in Iran, J. Soc. Serv. Res. 45 (2) (2019) 151–165.
[73] H. Oh, H.J. Kim, M.S. Mehboob, J. Kim, Y. Kim, Sources and uncertainties of future global drought risk with ISIMIP2b climate scenarios and socioeconomic indicators, Sci. Total Environ. 859 (2023) 160371.
[74] G.G. Ribeiro Neto, L.A. Melsen, E.S. Martins, D.W. Walker, P.R. Van Oel, Drought cycle analysis to evaluate the influence of a dense network of small reservoirs on drought evolution, Water Resour. Res. 58 (1) (2022) e2021WR030799.
[75] W.Z. Shi, S.Z. Huang, K. Zhang, B.J. Liu, D.F. Liu, Q. Huang, W. Fang, Z.M. Han, L.J. Chao, Quantifying the superimposed effects of drought-flood abrupt alternation stress on vegetation dynamics of the Wei River Basin in China, J. Hydrol. 612 (2022) 1–14.
[76] P.Y. Chen, A.A. Dagestani, Urban planning policy and clean energy development Harmony- evidence from smart city pilot policy in China, Renew. Energy 210 (2023) 251–257.
[77] W.Q. Liang, H.H. Wang, H.Y. Xue, Y.D. Chen, Y.H. Zhong, Spatiotemporal characteristics and co-effects of air quality and carbon dioxide emissions changes during the COVID-19 epidemic lockdown measures in China, J. Clean. Prod. 414 (2023) 137755.
[78] S. Koley, Sustainability appraisal of arsenic mitigation policy innovations in West Bengal, India, Infrastructure Asset Management 10 (1) (2022) 17–37.
[79] P. Samuels, S. Huntington, W. Allsop, J. Harrop (Eds.), Flood Risk Management: Research and Practice: Extended Abstracts Volume (332 Pages)+ Full Paper CD-ROM, CRC Press, 2008.
[80] D. Wilhite, R.S. Pulwarty (Eds.), Drought and Water Crises: Integrating Science, Management, and Policy, CRC Press, 2017.
[81] J. Lu, L. Ren, C. Zhang, D. Rong, R.R. Ahmed, J. Streimikis, Modified Carroll's pyramid of corporate social responsibility to enhance organizational performance of SMEs industry, J. Clean. Prod. 271 (2020) 122456.
[82] X. Zeng, J. Zhao, D. Wang, X. Kong, Y. Zhu, Z. Liu, G. Huang, Scenario analysis of a sustainable water-food nexus optimization with consideration of population-economy regulation in Beijing-Tianjin-Hebei region, J. Clean. Prod. 228 (2019) 927–940.
[83] A. Waheed, T. Bernward Fischer, M.I. Khan, Climate change policy coherence across policies, plans, and strategies in Pakistan—implications for the China–Pakistan economic corridor plan, Environ. Manag. 67 (2021) 793–810.
[84] H. Kreibich, A.F. Van Loon, K. Schröter, P.J. Ward, M. Mazzoleni, N. Sairam, G. Di Baldassarre, The challenge of unprecedented floods and droughts in risk management, Nature 608 (7921) (2022) 80–86.

[85] J.K. Kamara, B.W. Sahle, K.E. Agho, A.M. Renzaho, Governments' policy response to drought in Eswatini and Lesotho: a systematic review of the characteristics, comprehensiveness, and quality of existing policies to improve community resilience to drought hazards, Discrete Dynam Nat. Soc. 2020 (2020) 1–17.

[86] S.H. Chen, Reflection on the specialization transformation of emergency management mechanism, Chinese Journal of Emergency Management 2020 (3) (2020) 30–33.

[87] A.A. Dagestani, L. Qing, M. Abou Houran, What remains unsolved in sub-African environmental exposure information disclosure: a review, J. Risk Financ. Manag. 15 (2022) 487.